

Impact of morphological change of a regulated gravel-bed river on downstream fish habitat following a flood

Jiyeon Jang ^a, Byungwoong Choi ^b, Sung-Uk Choi ^{a,*}

^a Department of Civil and Environmental Engineering, Yonsei University, Republic of Korea

^b National Institute of Environmental Research, Republic of Korea

ARTICLE INFO

Keywords:

Physical habitat simulation
Morphological change
Hydro-morphodynamic simulation
Regulated river
Gravel-bed river
Substrate

ABSTRACT

Global climate change has led to recurring severe floods and droughts. Severe floods can alter the extent of river morphology, which is crucial to the river ecosystem. Morphological changes in rivers have been largely overlooked in conventional assessments of fish habitats. This study presents physical habitat simulations to investigate the impact of morphological change after a flood on fish habitats in a regulated river, using a hydro-morphodynamic model. The study reach is a 12.8 km long gravel-bed reach in the Geum-gang River, Korea. It consists of a series of bends, located downstream of the Yongdam Dam. For the physical habitat simulations, the most dominant and endemic fish species was selected as the target fish. The HEC-RAS 1D model and habitat suitability curves were used for hydro-morphodynamic and habitat simulations, respectively. The hydro-morphodynamic simulation provides information on changes in river morphology and substrate, as well as flow depth and velocity. The physical habitat simulation reveals that the quality of physical habitats for the target fish deteriorates after the flood due to increased water depth, which is associated with erosion along the study reach. This study demonstrates the potential of hydro-morphodynamic simulation for designing a sediment replenishment scheme to restore fish habitat downstream of dams.

1. Introduction

Global climate change is becoming increasingly evident, resulting in severe floods and droughts that repeatedly occur worldwide. Large-scale river works have been carried out for flood control and the expansion of cities and transportation. Urbanization and floodplain land use have been issues in both developed and developing countries. All over the world, white rivers have changed to green mainly due to anthropogenic activities (Woo, 2010). These provide the main drivers of the change in river morphology.

River morphology presents the spatial framework for all fish habitats (Kellerhals and Miles, 1996). However, river morphology has been treated less importantly than other habitat variables, such as velocity and flow depth, particularly in physical habitat simulations (Choi et al., 2017; Kim and Choi, 2021). The conventional perspective on river morphology concerning physical habitat simulation was relatively simple. For instance, it was thought that channel aggradation occurs due to increased slope, increased sediment load, and flow regulation. This might come from Lane's law, such as $Q_s/Q \propto S/d_{50}$ (here, Q_s = sediment load, Q = discharge, S = channel slope, and d_{50} = median size of bed

sediment). This law appears to be qualitatively sound, but its validity has rarely been quantitatively proven. Instead, the literature shows that damming results in reservoir sedimentation, downstream armoring, and channel degradation due to reduced sediment supply from the dam (Simon et al., 2002; Choi et al., 2005).

Morphodynamic change affects fish habitats in two ways. One is the morphological change or riverbed elevation change in a 1D sense. Sediment transport by high flows induces sedimentation or erosion in the river reach, changing flow depth and velocity. The other is the change in substrate, which can have a more serious effect on fish habitats than the first (Kellerhals and Miles, 1996; Servanzi et al., 2024; White et al., 2025). For example, downstream of instream installations, the riverbed coarsens, primarily due to the blockage of fine sediment transport. To assess this latter impact, detailed information on the fish species' substrate preferences is necessary.

Despite its potential importance, river morphology in reaches downstream of a dam has been addressed in physical habitat simulations only recently. Parra et al. (2024) investigated changes in river morphology and fish *meso* habitats following an experimental flood in the lower Spol River, Switzerland. They used a model integrating

* Corresponding author.

E-mail address: schoi@yonsei.ac.kr (S.-U. Choi).

morphodynamics, hydraulics, sediment transport, and habitat for the analysis. Para et al. found little correlation between changes in the channel morphology and inhabitant suitability. Still, they indicated that integrating morphodynamics and eco-hydraulic analysis is relevant to support the implementation of flow restoration programs. Duffin et al. (2023) studied the impact of restoring unregulated flows on fish habitats. They applied a quasi-steady, quasi-3D solver for hydraulic, sediment transport, and morphodynamic simulations to the Lemhi River in Idaho, US. Duffin et al. found that hydrologic restoration can improve subdued topography. However, its impact can be limited when applied to a straightened channel lacking bedforms or sinuosity. Yang et al. (2023) carried out physical habitat simulations to assess the habitat quality after releasing high flow from the Rumei Dam in Lancang River, China. They used a 2D model for hydraulic and morphological simulation and HSCs for habitat simulation, respectively. Yang et al. found that the dam severely degrades downstream fish habitats, but sediment replenishment can help restore fish habitat fragmentation.

A problem with an upstream dam is reduced sediment supply. The dam blocks most of the sediment supply to the downstream reach. As a result, the riverbed degrades and the bed sediment downstream of the dam coarsens over time. The research question of what impact flood-induced morphological changes would have on downstream fish habitats in this altered river environment motivated this study.

This study investigated morphological changes in a gravel-bed river downstream of a dam and assessed their impact on fish habitat following a large flood. The study area is located downstream of the Yongdam Dam in the Geum-gang River, Korea. For the physical habitat simulation, the HEC-RAS 1D model and HSCs were used for hydro-morphodynamic and habitat simulations, respectively. The most dominant and endemic fish species was selected as the target fish. The hydro-morphodynamic model was validated for flow and changes in river morphology and substrate in the study area. A physical habitat simulation was conducted for the target fish species, and the impact of morphological changes following the flood on the physical habitat was assessed.

2. Materials and methods

2.1. Study area

The study area is a 12.8 km long reach in the Geum-gang River, Korea (see Fig. 1). The study reach extends from immediately downstream of the Yongdam Dam to the Daeti-gyo Bridge. The study reach is a gravel-bed river. The average slope of the study reach is 0.0015. As shown in the figure, the reach downstream of the dam exhibits serious meandering, characterized by a series of channel bends. The study reach is regulated by the upstream dam, which releases water for hydropower

generation throughout the year, except during floods. The flood season in Korea usually is from June to August. The discharges for drought flow (Q_{355}), low flow (Q_{275}), normal flow (Q_{185}), and averaged-wet flow (Q_{95}) are 2.87, 5.73, 9.51, and $17.13 \text{ m}^3/\text{s}$, respectively (Ministry of Land, Infrastructure, and Transport, 2011). Here, Q_n denotes the average flow discharge that is exceeded on n days of the year.

The Geum-gang River, the third-largest river in Korea, flows through the central part of the Korean Peninsula. The watershed area is approximately 9900 km^2 , accounting for about 9 % of the total area of Korea. The Geum-gang River has more than 21 major tributaries. The river is 397.8 km long with an average slope exceeding 0.001 in the upstream reach. The Yongdam Dam is located on the upper reach of the Geum-gang River, Korea. It is a multipurpose dam, completed in October 2001. The dam is 70 m high and 500 m wide, with a total water storage capacity of approximately $8.15 \times 10^8 \text{ m}^3$. Key facilities include a 21.9 km-long water-conveyance tunnel and a flow-diversion hydropower plant at the tunnel's end. The Yongdam Dam is the 5th largest dam in Korea.

We selected the study site because the study reach has experienced degradation and armoring after the construction of the upstream dam. Moreover, the data for investigating previous morphodynamic changes were available.

2.2. Data

The flow computation requires the discharge and stage at the upstream and downstream boundaries, respectively. For the upstream boundary condition, the hourly-averaged discharge released from the Yongdam Dam was used (K-water, 2023). The stage data measured hourly at the Daeti-gyo Bridge Station (Geum River Flood Control Office (GRFCO), 2023) were used for the downstream boundary condition.

Bed sediment was sampled at 13 sites spaced 1 km apart in the study reach. Bed sediment consists of sand, gravel, and cobble. The median size of the bed sediment is 23.3 mm, indicating a gravel-bed river.

Fig. 2(a) shows the discharge from Yongdam Dam from 2011 to 2022 (K-water, 2023). Values of the peak discharges are given in the figure. It can be seen that a large amount of discharge was released through the dam gates only 5 times over the last 11 years. The largest flood during this period occurred in 2020, with a peak discharge of $2904 \text{ m}^3/\text{s}$.

Fig. 2(b) shows the longitudinal profiles of bed elevation measured in 2011 and 2022 (Ministry of Land, Infrastructure, and Transport, 2011; Ministry of Environment, 2022). In the figure, the upstream boundary at $x = 0 \text{ km}$ is located immediately downstream of the dam, and the downstream end is the Daeti-gyo Bridge, 12.8 km from the dam. The bed elevation was measured at the thalweg of the channel cross-section. Both profiles show vertical fluctuations severely. This is thought to

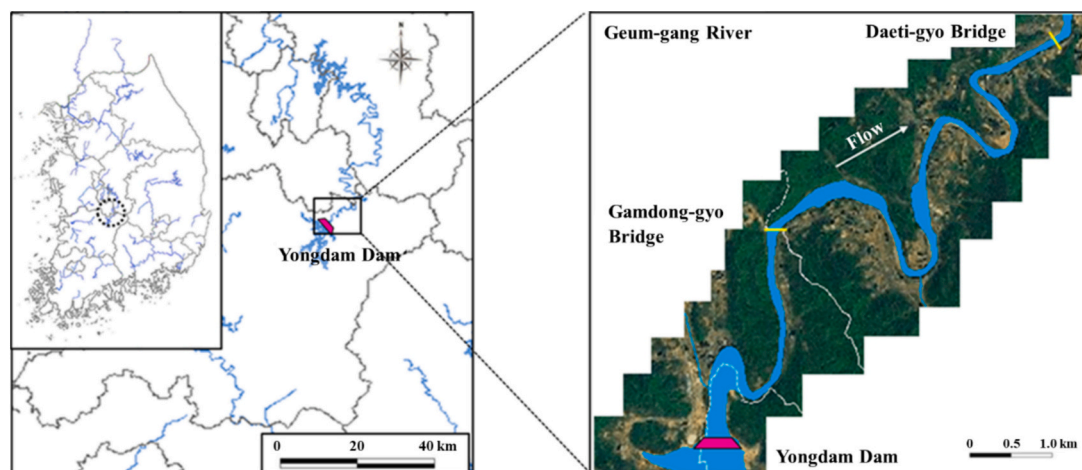


Fig. 1. Study reach.

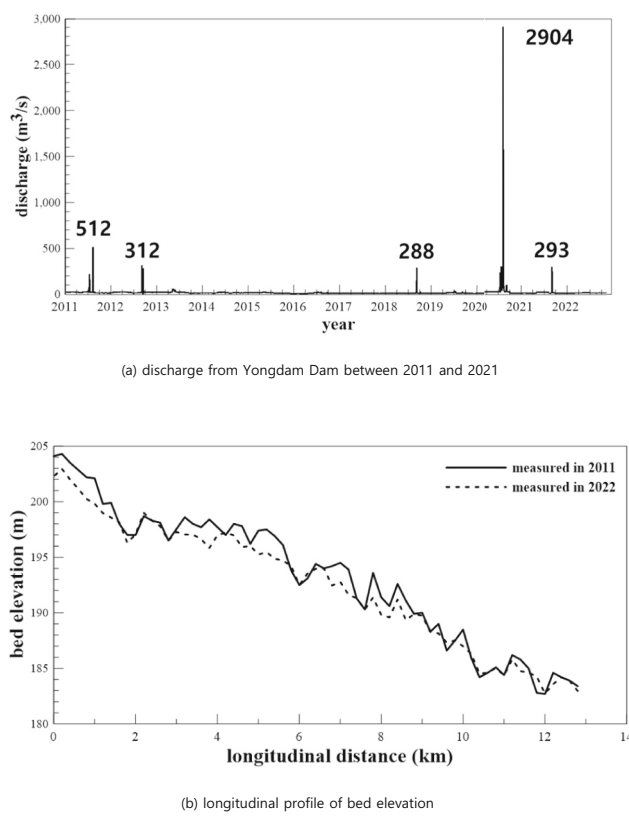


Fig. 2. Discharge and bed elevation.

result from the pool-riffle sequence, which is related to the river's meandering characteristics. Overall degradation has occurred in the study reach since 2011, as is typical in the reach downstream of a dam (Choi et al., 2005). The maximum erosion in the study site ranges from 2.0 to 2.3 m at several locations, including 1.0, 5.0, and 7.2 km from the dam.

2.3. Fish dominance

Fig. 3 illustrates the distribution of dominant fish species as determined by field monitoring in the study area (Jung, 2018). The field monitoring for fish species was carried out in September and October 2017. It was found that *Zacco koreanus* was the most dominant fish,

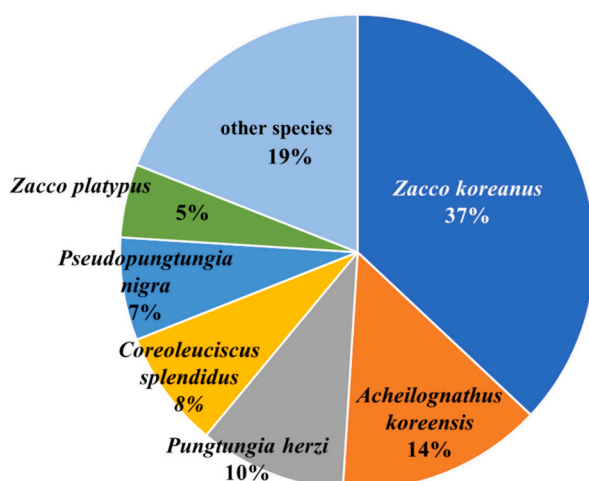


Fig. 3. Distribution of dominant fish in the study reach.

followed by *Acheilognathus koreensis*, *Pungtungia herzi*, *Coreoleuciscus splendidus*, *Pseudopungtungia nigra*, *Zacco platypus*, etc. Among these dominant fish species, *Zacco koreanus*, *Acheilognathus koreensis*, *Coreoleuciscus splendidus*, and *Pseudopungtungia nigra* are endemic fish species, and *Pseudopungtungia nigra* is endangered species. It is noticeable that the first two dominant fish species, namely *Zacco koreanus* and *Acheilognathus koreensis*, account for approximately 50 % of the total fish species.

2.4. Hydro-morphodynamic simulation

In the present study, the HEC-RAS 1D model (USACE, 2024) was used for hydro-morphodynamic simulation. The governing equations for the flow are given by

$$\frac{\partial A}{\partial t} + \frac{\partial Q}{\partial x} - q_l = 0 \quad (1)$$

$$\frac{\partial Q}{\partial t} + \frac{\partial(VQ)}{\partial x} + gA \left(\frac{\partial z}{\partial x} + S_f \right) = 0 \quad (2)$$

which are the continuity and momentum equations, respectively. In Eqs. (1) and (2), x is the distance in the flow direction, t is the time, A is the cross-sectional area, Q is the discharge, q_l is the lateral discharge (per unit length), V is the flow velocity, g is the gravitational acceleration, and S_f is the friction slope.

The morphological change in a river can be accounted for by solving Exner's equation such as

$$\frac{1}{1 - \lambda} \frac{\partial Q_s}{\partial x} + B \frac{\partial z}{\partial t} = 0 \quad (3)$$

where λ is the porosity, Q_s is the sediment load, B is the width of the mobile bed, and z is the bed elevation from a certain datum.

2.5. Habitat simulation

Habitat simulation provides habitat suitability information on physical habitat variables such as velocity, flow depth, and substrate. Typically, as noted by Boavida et al. (2013), hydraulic simulations provide velocity and flow depth, while the substrate is assessed through field monitoring. However, information on all three variables can be given if the hydro-morphodynamic simulation is carried out with proper initial conditions.

The habitat suitability is expressed by the composite suitability index (CSI). In the present study, to compute the CSI, the following multiplicative aggregation method is used (Bovee et al., 1998):

$$CSI = f(V) \times f(H) \times f(s) \quad (4)$$

where $f(HV)$ is the habitat suitability value for each habitat variable HV . Here, HV includes velocity V , flow depth H , and substrate s . The CSI ranges from 0 to 1, representing the worst and best habitat conditions, respectively.

Both the expert-knowledge and data-driven models are used for habitat simulation. The habitat suitability curves (HSCs), which are most widely used, belong to the expert-knowledge model. The primary drawback of this type of model is that habitat suitability is influenced by experts' subjective opinions. The data-driven model includes artificial neural network (ANN) models, fuzzy logic, statistical methods, and genetic algorithms (Choi and Choi, 2018; Im et al., 2019). In the present study, despite its drawbacks, the HSCs is used for habitat simulation due to the limited availability of monitoring data.

The Weighted Usable Area (WUA) is calculated using the CSI distribution. The WUA is the total area of the available habitat for the target fish species in the study area. The WUA, representing the overall wetted area weighted by CSI values, can be calculated as (Bovee et al., 1998)

$$WUA = \sum_{i=1}^k CSI_i \times A_i \quad (5)$$

where k is the total number of cells and A_i is the area of the i -th cell.

Fig. 4 shows the Habitat Suitability Curves (HSCs) for the target fish, *Zacco koreanus*. *Zacco koreanus* is an endemic species that only inhabits rivers in Korea. It can be seen that the target fish prefer flow depths and velocities in the ranges of 0.16–0.42 m and 0.01–0.26 m/s, respectively. This indicates that *Zacco koreanus* is a lentic fish, which prefers a slowly flowing aquatic environment. *Zacco koreanus* is known to inhabit flow over gravel and cobble, specifically, substrates 5 and 6, with particle sizes ranging from 2 to 64 mm and 64 to 250 mm, respectively (Ministry of Land, Infrastructure, and Transport, 2011; Hur et al., 2009; Kang, 2012). Since the substrate of the study reach consists of gravel, as stated earlier, the substrate as a habitat variable is not considered in the physical habitat simulation.

2.6. Validation of hydro-morphodynamic model

Validation of the hydro-morphodynamic model was conducted for both the flow and river morphology. Here, the model validation is given for computing the morphological change first. The morphological change of the study reach is calculated over the period 2011–2021. The discharge hydrograph at the upstream boundary is shown in Fig. 2(a), where five major floods are observed. The stage data measured at the Daeti-gyo Station were imposed at the downstream boundary. The 2011 data, shown in Fig. 2(b), were used as the initial bed elevation. For bed sediment, particle size distributions measured at 13 sites in 2011 (see

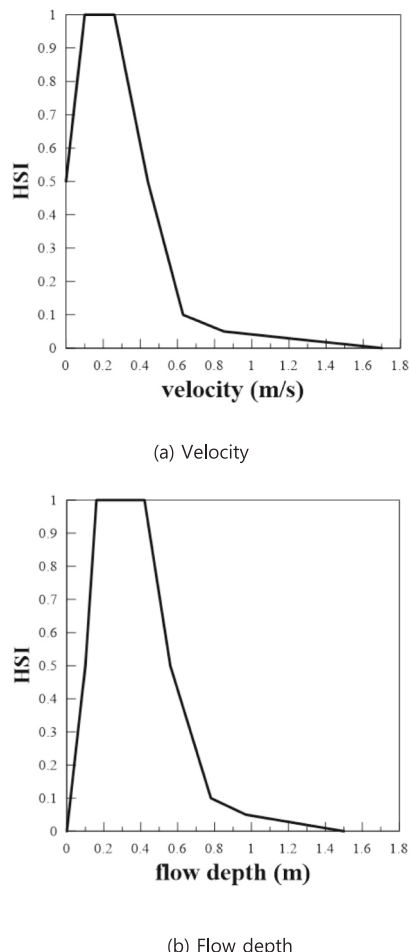


Fig. 4. Habitat suitability Curves for *Zacco koreanus*.

Fig. 6) were used.

Fig. 5 shows the computed longitudinal bed elevation profile, along with the measured data. It was assumed that sediment supply from the dam was negligible. Four total sediment load formulas were tested, including Meyer-Peter and Muller's, Engelund-Hansen's, Ackers-White's, and Yang's formulas (see Supplementary Materials). They resulted in Root Mean Square Errors (RMSEs) of 0.90, 0.72, 0.88, and 0.87 m, respectively. Thus, in the present study, Engelund-Hansen's formula was used for the sediment transport in the study reach. The computed bed elevation is in relatively good agreement with the measured data. However, the degradation in the reaches for $6 \text{ km} < x < 7 \text{ km}$ and $8 \text{ km} < x < 10 \text{ km}$ is slightly over-predicted.

Fig. 6 shows the particle size distributions obtained at 12 different sites in 2011 and 2022. The computed distributions in 2022 are also provided for comparison. The data measured at $x = 10 \text{ km}$ in 2022 include errors, so they were excluded from the comparison. The computed distribution agrees moderately well with the measured data, except at the site $x = 12 \text{ km}$ from the dam. A general trend observed in the particle size distribution is that bed sediment particles have been coarsened during this period. However, the distribution measured at $x = 12 \text{ km}$ in 2022 indicates that bed particles have become finer during the same period. Nonetheless, this figure demonstrates that the hydro-morphodynamic model can simulate not only changes in bed elevation but also changes in bed sediment. In the figure, it is also noteworthy that armoring of bed sediment occurred in the study reach during 2011 and 2022. The median size of bed sediment changed from 7.7 mm to 23.3 mm during this period.

The distribution of the sorting coefficient with the longitudinal distance is plotted in Fig. 7. The sorting coefficient (s_0), defined by $\sqrt{d_{75}/d_{25}}$, indicates the level of uniformity in the particle size distribution. For natural sediment, the sorting coefficient ranges in the range of $2.0 < s_0 < 4.5$ (Woo, 2001). A higher sorting coefficient indicates that particles are more widely distributed. The coefficients calculated from data measured in 2011 and 2022 are given. It can be observed that the particles of bed sediment have become remarkably uniform by 2022. The sorting coefficient averaged over the study reach is 4.05 in 2011 and 2.35 in 2022. The sorting process of bed sediment downstream of the dam occurred due to bed armoring, with the flow carrying away fine particles. Notably, the 2011 data indicate that bed armoring occurred up to 3 km downstream from the dam. This seems reasonable, considering the dam was completed in 2001.

For model validation of the flow, computations were performed for the August 2020 flood. The discharge and stage hydrographs in Fig. 8(a) were imposed at the upstream and downstream boundaries, respectively. The stage data were measured at the Daeti-gyo Bridge in Fig. 1. In 2020, the maximum discharge of $2904 \text{ m}^3/\text{s}$, which is close to the 200-year flood of $2920 \text{ m}^3/\text{s}$, occurred on August 8, 2020. For the roughness coefficient, the entire study reach was divided into two. That is, a roughness coefficient of $n = 0.065$ was used in the upper reach to Gamdong-gyo Bridge, located 4.6 km from the dam, and $n = 0.035$ in the

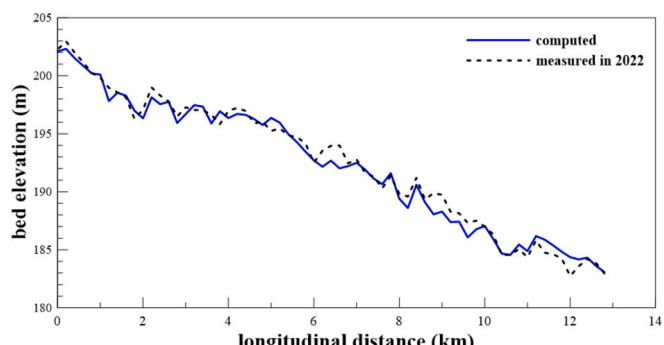


Fig. 5. Comparison between computed bed elevation and measured data.

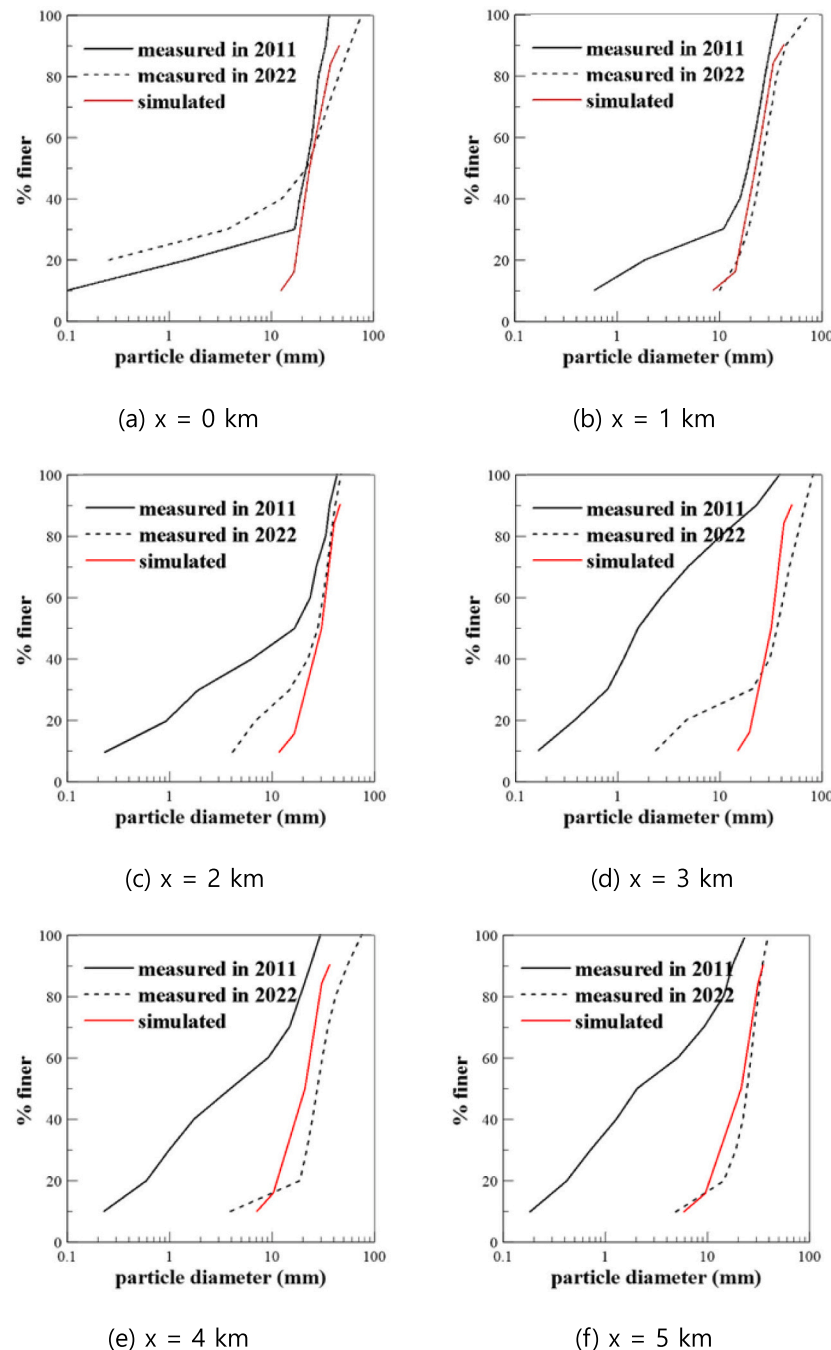


Fig. 6. Particle size distribution of bed sediment.

lower reach downstream from the Gamdong-gyo Bridge (see Fig. 1). These roughness coefficient values were suggested by the [Ministry of Land, Infrastructure, and Transport \(2011\)](#). This is thought to be reasonable because the plot of the median size of bed sediment in Fig. 6 shows higher values in the upper reach, although not shown herein.

Fig. 8(b) compares the computed stage with the measured data at Gamdong-gyo Station. The maximum difference of approximately 0.4 m occurred during the falling stage of the flood, specifically between August 9 and August 10. However, the overall prediction is successful, indicating that the hydro-morphodynamic model can predict floods with reasonably good accuracy.

3. Results

Now, the Impact of morphological change on downstream fish habitat is investigated. It is assumed that the same flood as shown in Fig. 8, which is close to the 200-year flood, occurs in the study reach. The bed elevation profile measured in 2022, as shown in Fig. 5, and the particle size distribution of bed sediment measured in 2022, as depicted in Fig. 6, are used as initial conditions.

Fig. 9(a) shows the computed bed elevation after the flood with the initial bed elevation profile. For sediment transport, the Engelund-Hansen formula was used, with no sediment load specified at the upstream boundary. Previously, the Engelund-Hansen formula was proposed for predicting total sediment load in large rivers in Korea (Choi

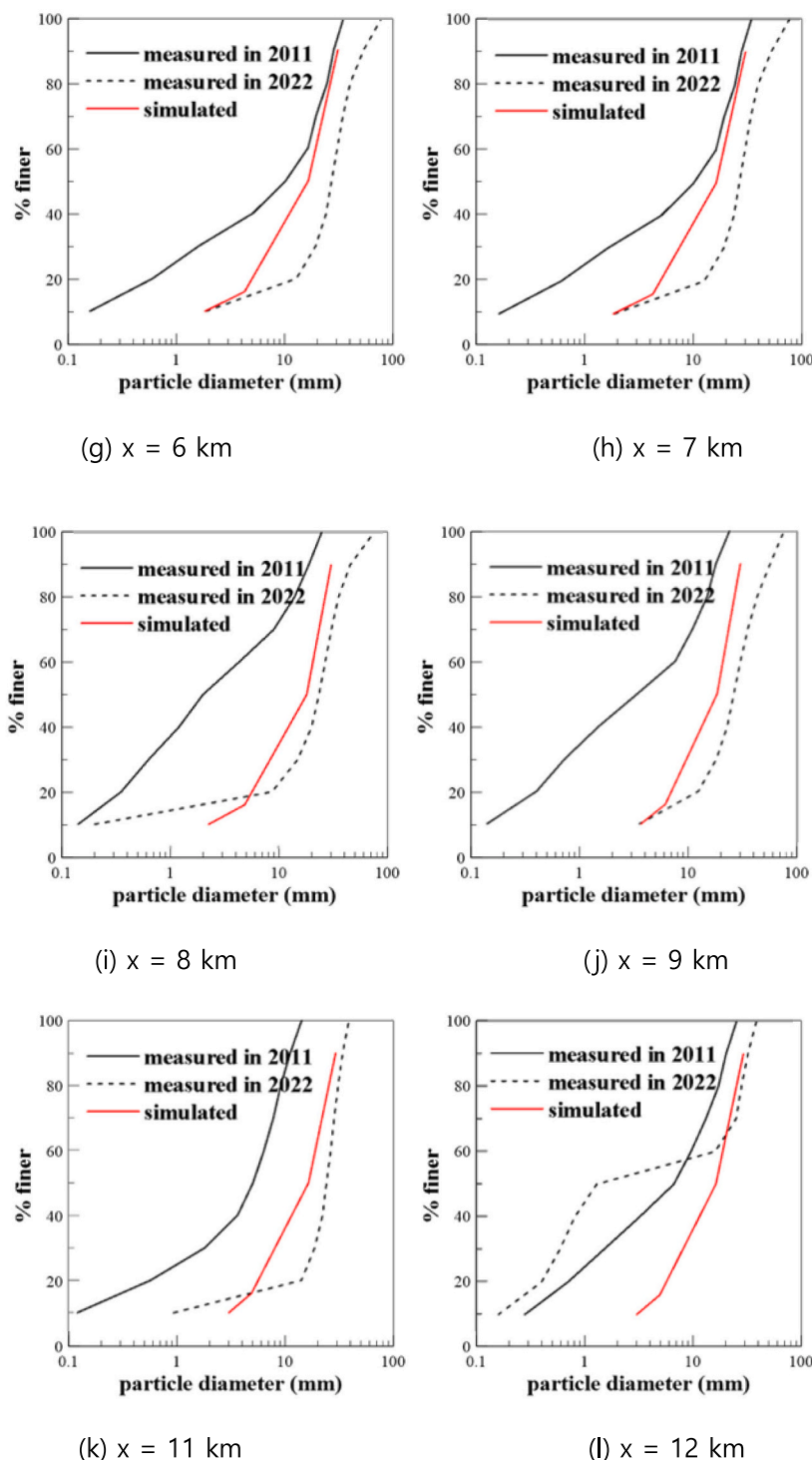


Fig. 6. (continued).

and Lee, 2015). Overall, degradation occurs in the study reach. The figure shows that more erosion occurs in the upper reach than in the lower reach, which is typical of the riverbed downstream of a dam. A similar type of erosion has been observed in a reach downstream of the Daecheong Dam, Korea (Woo, 2001). The sediment supply from the dam is significantly reduced, and the upper reach for $0 < x < 5$ km is directly exposed to the tractive force. This resulted in coarse bed sediment or a higher roughness coefficient in the upper reach, as observed. However, such erosion does not occur in the lower reach for $5 < x < 12.8$ km, suggesting a balance between sediment inflow and outflow. The average

depth of erosion per unit width is 1.82 m in the upper reach and 1.05 m in the lower reach.

For the regulated flow of $Q = 8.7 \text{ m}^3/\text{s}$ released from the dam for hydropower generation, the flow depth and velocity are $H = 0.44 \text{ m}$ and $V = 0.11 \text{ m/s}$, respectively, at a location immediately downstream from the dam. With the average slope of $S_0 = 0.0015$ and particle diameter of $d = 20.7 \text{ mm}$, the particle Reynolds number ($\text{Re}_p = \sqrt{Rg}d/\nu$, here, R =submerged specific gravity of sediment, and ν =kinematic viscosity of water) and corresponding Shields parameter ($\tau^* = HS_0/(Rd)$) become $\text{Re}_p = 12,000$ and $\tau^* = 0.019$, respectively. The computed Shields

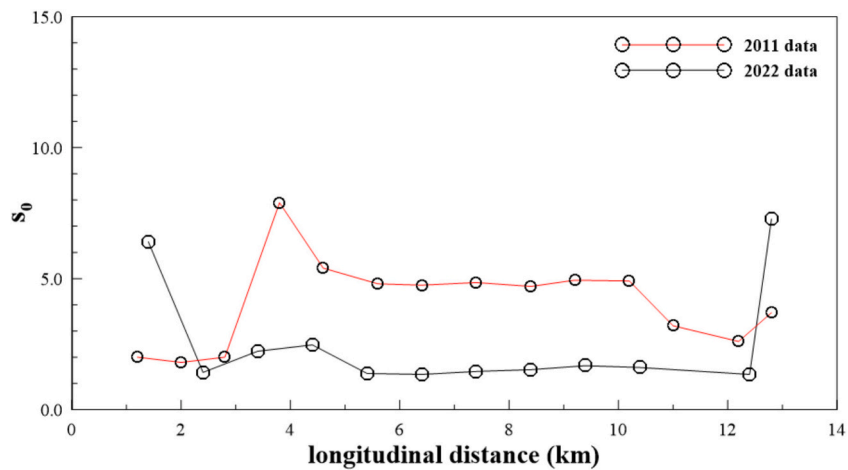
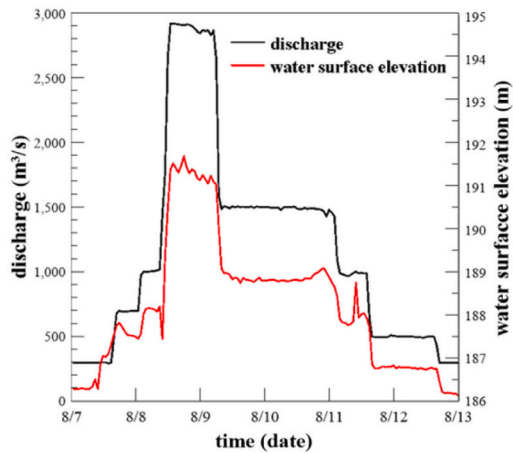
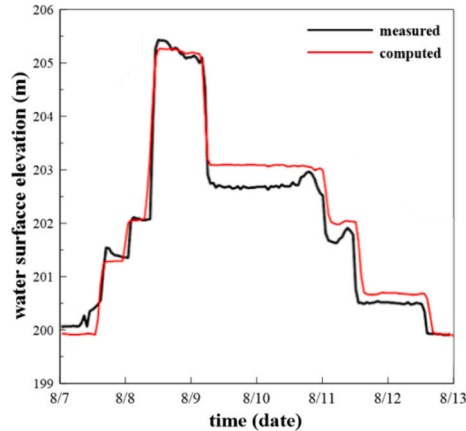


Fig. 7. Distribution of sorting coefficient.



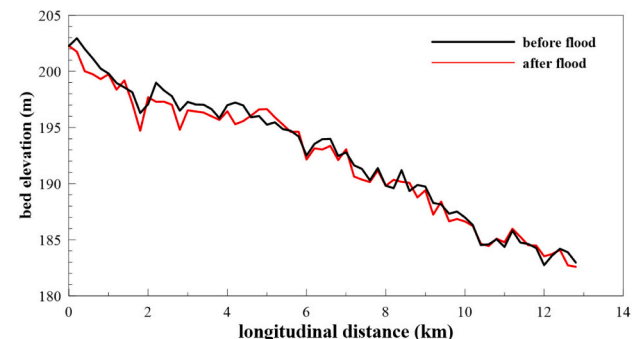
(a) Discharge hydrograph in 2020



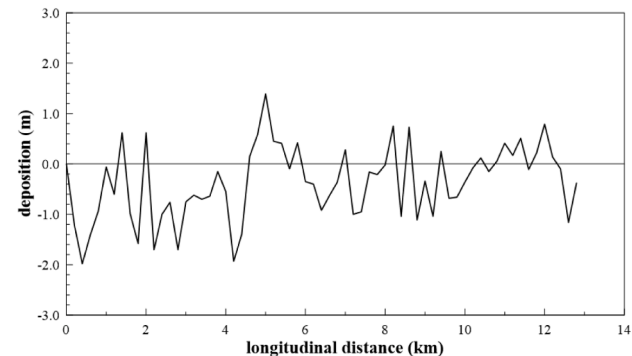
(b) Measured and computed water surface elevation at Gamdong-gyo Bridge Station

Fig. 8. Validation of flow computation.

parameter is smaller than the critical value of 0.06, indicating that this regulated flow does not transport bed sediment particles. If the discharge is increased to the peak flow of $Q = 2900 \text{ m}^3/\text{s}$ during the 2020 flood, the Shields parameter becomes $\tau^* = 0.329$, which is larger than the critical value. This simple calculation shows that bed sediment



(a) Morphological change after the flood



(b) Sediment deposition after the flood

Fig. 9. Morphological change and sediment deposition after the flood.

can rarely be transported by the regulated flows; however, it can be transported during floods in the study reach.

Fig. 9(b) shows the amount of sediment deposition averaged over the width of the cross-section. In the figure, the negative deposition means erosion of the bed. The figure shows that erosion and deposition occur repeatedly along the study reach. This trend is similar to that in a meandering river reach computed by a three-dimensional numerical model in Parsapour-Moghaddam et al. (2019). However, the amount of erosion is much larger than that of deposition. In the figure, the maximum erosion of about 2.0 m occurs at 0.5 and 4.2 km from the dam, and the maximum deposition of 1.4 m occurs at $x = 5 \text{ km}$ from the dam.

The particle size distributions of bed sediment before and after the

flood are given in Fig. 10. The distributions are provided at every 2.0 km from the dam. Bed sediment particles are slightly coarser after the flood; however, the distributions before and after the flood appear similar overall. This is because the previous floods had caused bed armoring, and the dam blocks further sediment supply. The particle size distributions for $0 < x < 3$ km, including fine particles, as shown in Fig. 6, become very uniform as fine particles flow out from the bed after the flood. The median size of the bed sediment particles changes from 22.8 mm to 24.1 mm due to the flood. In addition, the sorting coefficient of the bed sediment particles changes from 2.44 (2.35) to 1.84 after the flood. This indicates that the bed sediment particles become uniform after the flood, but the change is less severe than before.

The CSI distribution for the regulated flow of $Q = 8.7 \text{ m}^3/\text{s}$ is given in Fig. 11(a). Since the interval of the hydrographic survey in the study reach is 200 m, the CSI distribution within this interval is uniform, as shown in the figure. Two distinct features are observable in Fig. 11(a). First, the CSI fluctuates in the longitudinal direction, which is related to the fluctuations of the bed elevation profile, as shown in Fig. 2(b). Secondly, the CSI peak value decreases in the longitudinal direction. A similar pattern is observed before the flood, indicating that the quality of the physical habitats for *Zacco koreanus*, a lentic fish species, degrades continuously in the longitudinal direction. The WUA of the study reach before the flood was $339,443 \text{ m}^2$ with a total study area of $1,282,763 \text{ m}^2$, resulting in a WUA ratio of 0.265. This indicates that 26.5 % of the study

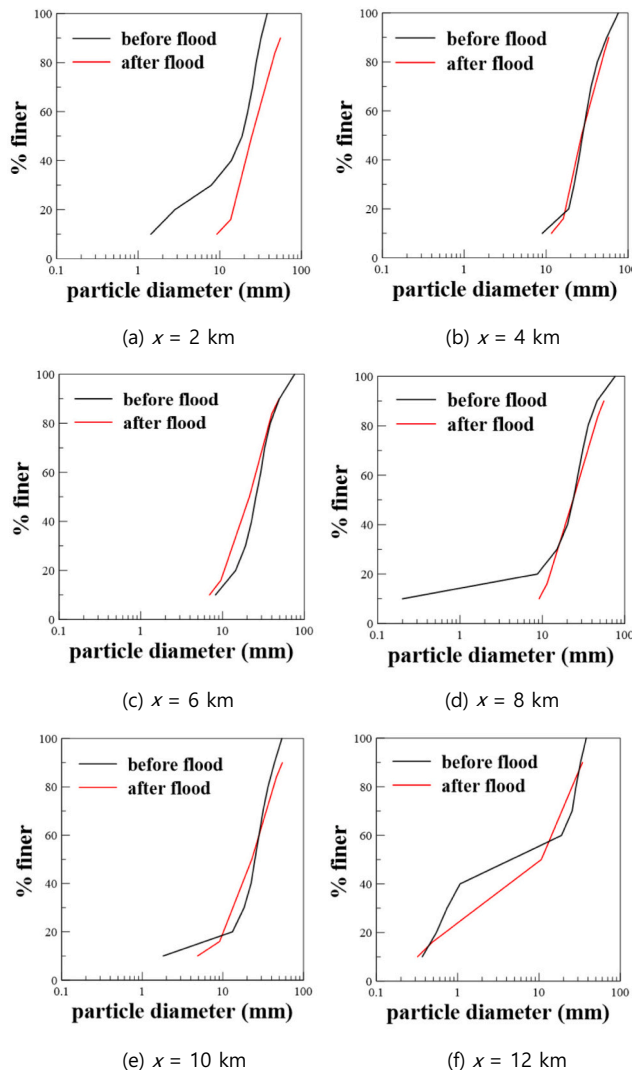


Fig. 10. Particle size distribution of bed sediment before and after the flood.

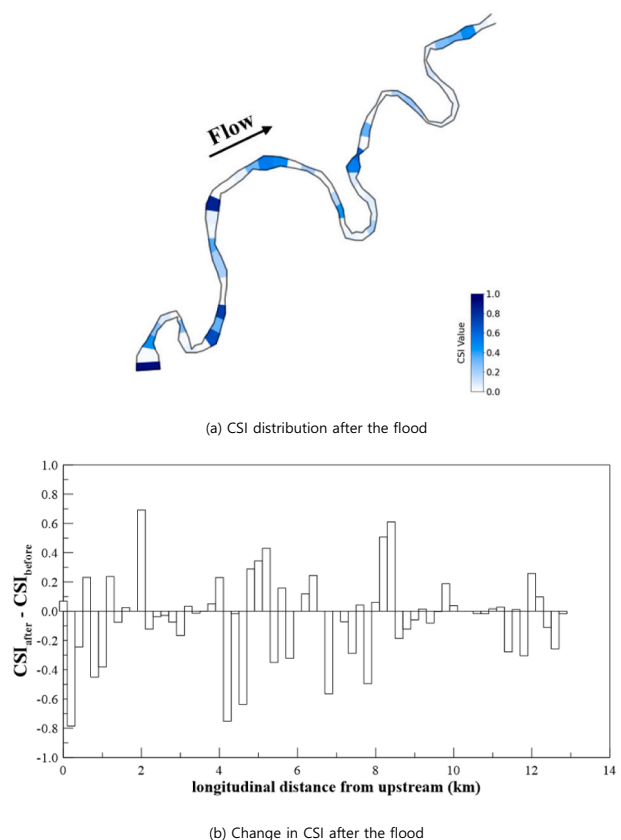


Fig. 11. CSI distribution and change in CSI after the flood.

area is appropriate for the habitats of the target fish. After the flood, the WUA of the study reach in Fig. 9(a) is $279,809 \text{ m}^2$ with a reduced WUA ratio of 0.218. This means the WUA decreases by 17.6 % due to morphological changes following the flood.

In Fig. 11(b), the changes in CSI after the flood are plotted in the longitudinal direction. The positive value on the vertical axis indicates that the physical habitat quality for the target fish improves after the flood. It can be observed that improvements and deteriorations in physical habitats occur repeatedly along the longitudinal direction. This is related to the morphological changes after the flood. In addition, the figure shows that the change in CSI in the upper reach is larger than that in the lower reach. This is due to the morphological change, as in Fig. 9(b). In most cases, CSI degradation after the flood is associated with increased flow depth over the entire reach. The quality of the physical habitats degrades primarily in the upper reach, where the flow depth increases due to erosion.

4. Discussion

Computing the morphological change of a river is a challenging task (Parker, 2004). The approaches for numerically simulating the morphological change of a river can be classified into three methodologies, depending on the spatial dimension of the flow model, namely 1D, 2D, and 3D models. The 1D model provides rough, averaged information on river morphology over the river reach, but cannot pinpoint the locations of morphological changes. However, both 2D and 3D models can provide microhabitats in physical habitat simulations (Boavida et al., 2013). The 2D model assumes horizontal flow, which is valid for shallow flow. To accurately predict morphological change, the 2D model must consider the effects of secondary flows and lateral slope (Lai, 2020). The 3D model is accurate, but it is expensive. Moreover, the morphological change computed by the 3D model is not remarkably precise compared

with the measured data (Khosronejad et al., 2011). Lai et al. (2022) attributed this to the fact that the estimation of turbulent bed shear stress is not accurate enough, and equilibrium sediment transport formulas are too empirical.

In Korea, a basic plan for river management is legally required to be established once every 10 years for rivers managed by the nation. The basic plan includes hydrogeographic survey data and the collection of bed sediment to examine morphodynamic changes in the river over the last 10 years. Typically, the hydrogeographic survey is conducted every 200 m along the river reach. The results of the hydrogeographic survey provide essential information on river degradation and aggradation, local riverbed erosion, and sediment deposition. However, the survey results do not provide sufficient information to identify changes in microhabitats. The present study analyzed morphological change using data from the basic plan (Ministry of Land, Infrastructure, and Transport, 2011; Ministry of Environment, 2022), which provided a rationale for using the 1D hydro-morphodynamic model.

The physical habitat simulation generally uses habitat variables such as velocity, flow depth, and substrate. The velocity and flow depth are obtained from the hydraulic simulation, but the substrate is not. The habitat suitability for the substrate is evaluated based on field data. However, suppose the hydraulic simulation is replaced with a hydro-morphodynamic simulation, as in the present study. In that case, the simulation can provide not only changes in flow but also in river morphodynamics. Morphodynamic change encompasses morphological changes in a river and changes in the substrate composition, both of which affect the quality of fish habitats. In the present study, the change in substrate simulated by the hydro-morphodynamic model was not considered because the data indicate that the target fish prefer substrates larger than gravel. However, this study demonstrates the potential of hydro-morphodynamic computation for the computed substrate in physical habitat simulations.

Once a dam is built upstream, sediment supply from the dam is seriously reduced. Consequently, the downstream riverbed is exposed to degradation and armoring. This study reveals that WUA decreased by 17.6 %, suggesting deterioration of fish habitats due to morphological changes following the floods. The extent of deterioration by the change in substrate might be more serious, as indicated by Kellerhals and Miles (1996). That is, downstream aquatic animals may suffer a lack of fine particles. One countermeasure being implemented in the fields is sediment replenishment, supplying sediment in the reach downstream of a dam. To achieve this, sediment must be excavated from upstream locations where it was deposited and transported downstream. When a flood occurs, sediments that have been stacked on either the floodplain or main channel are flushed downstream of the dam. The hydro-morphodynamic simulations can be effectively used to design sediment replenishment plans to restore fish habitat by precisely delivering fine sediment particles downstream of dams.

5. Conclusions

This study investigated the morphological changes of a gravel-bed river reach regulated by an upstream dam and their impact on downstream fish habitats following a 200-year flood. A physical habitat simulation was conducted for the target fish species, *Zacco koreanus*. Hydro-morphodynamic and habitat simulations were performed using the HEC-RAS 1D model and HSCs, respectively. The hydro-morphodynamic model was validated by comparing the computed flow, river morphology, and bed sediment distribution with measured data. *Zacco koreanus*, the most dominant and endemic fish species, was selected as the target fish. In the present study, the substrate was not used as a habitat variable. This is because the study reach is a gravel-bed river with no discernible differences in the preferences of the target fish species.

Simulation results indicated that severe erosion occurred after the flood. The average erosion depth in the upper reach upstream of the

Gamdong-gyo Bridge was 73 % more than that in the lower reach downstream of the bridge. This is a typical pattern of the morphological change in the riverbed downstream of a dam. Furthermore, erosion of the bed and sediment deposition were found to occur repeatedly along the longitudinal direction, resulting in much greater erosion than deposition over the study area.

The CSI distribution after the flood also shows a fluctuating pattern in the longitudinal direction, with peak values decreasing in the same direction. These characteristics, also observed before the flood, indicate that the physical habitats of the target fish species degrade slowly along the longitudinal direction. The change in the CSI revealed that improvements and deterioration in the physical habitats occur repeatedly along the longitudinal direction, and the overall quality of the physical habitats degraded in the reach where flow depth increases due to erosion. This results in a 17.6 % decrease in the WUA within the study reach after the flood.

This study presented a physical habitat simulation in which hydraulic simulation is replaced by hydro-morphodynamic simulation. The hydro-morphodynamic simulation provided changes in river morphology and composition of bed sediment, as well as velocity and flow depth. This study revealed that morphological changes following the flood significantly reduced the quality of the physical habitats in the study area. Likewise, changes in substrate can affect physical habitats to a similar extent. However, unfortunately, the change of substrate was not considered in the present study because the HSC for the substrate is not sufficiently sensitive.

CRediT authorship contribution statement

Jiyeon Jang: Writing – review & editing, Writing – original draft, Software, Methodology, Investigation, Formal analysis, Data curation. **Byungwoong Choi:** Writing – review & editing, Software, Methodology, Formal analysis, Data curation, Conceptualization. **Sung-Uk Choi:** Writing – review & editing, Writing – original draft, Supervision, Funding acquisition.

Declaration of competing interest

The authors declare that they have no known competing financial interests or personal relationships that could have appeared to influence the work reported in this paper.

Acknowledgements

This work was supported by the National Research Foundation of Korea (NRF) grant funded by the Korea Government (RS-2023-00253784).

Appendix A. Supplementary data

Supplementary data to this article can be found online at <https://doi.org/10.1016/j.ecoleng.2025.107863>.

Data availability

Data will be made available on request.

References

- Bovee, K. D., Lamb, B. L., Bartholow, J. M., Stalnaker, C. B., Taylor, J., Henricksen, J., 1998. Stream habitat analysis using the instream flow incremental methodology. USGS Information and Technical Report (No. USGSBRDITR19980004).
- Boavida, I., Santos, J.M., Katopodis, C., Ferreira, M.T., Pinheiro, A., 2013. Uncertainty in predicting the fish-response to two-dimensional habitat modeling using field data. River Res. Appl. 29, 1164–1174. <https://doi.org/10.1002/rra.2603>.
- Choi, S.-U., Lee, J., 2015. Prediction of total sediment load in Sand-Bed Rivers in Korea using lateral distribution method. JAWRA J. Am. Water Resources Assoc. 51, 214–225. <https://doi.org/10.1111/jawr.12249>.

Choi, B., Choi, S.-U., 2018. Impacts of hydropeaking and thermopeaking on the downstream habitat in the Dal River, Korea. *Eco. Inform.* 43, 1–11. <https://doi.org/10.1016/j.ecoinf.2017.10.016>.

Choi, S.-U., Yoon, B., Woo, H., 2005. Effects of dam-induced flow regime change on downstream river morphology and vegetation cover in the Hwang River, Korea. *River Res. Appl.* 21, 315–325. <https://doi.org/10.1002/rra.849>.

Choi, S.-U., Kim, S.K., Choi, B., Kim, Y., 2017. Impact of hydropeaking on downstream fish habitat at the Goesan Dam in Korea. *Ecohydrology* 10, e1861. <https://doi.org/10.1002/eco.1861>.

Duffin, J., Yager, E.M., Buffington, J.M., Benjankar, R., Borden, C., Tonina, D., 2023. Impact of flow regulation on stream morphology and habitat quality distribution. *Sci. Total Environ.* 878, 163016. <https://doi.org/10.1016/j.scitotenv.2023.163016>.

Geum River Flood Control Office (GRFCO), 2023. Water Level Data. Water Resources Management Information System. Available from: https://www.wamis.go.kr/wkw/vwl_dubwlobs.dz (accessed 24 October 2024).

Hur, J.-W., Park, J.-W., Kang, S.-U., Kim, J.-K., 2009. Estimation of fish fauna and habitat suitability index in the Geum River Basin. *Korean J. Environ. Ecol.* 23, 516–527.

Im, D., Choi, B., Choi, S.-U., 2019. Change in fish community composition following weir removal, field observations, and physical habitat simulations. *River Res. Appl.* 35, 1062–1071. <https://doi.org/10.1002/rra.3480>.

Jung, S.H., 2018. A Research on Estimation and Securing of Environmental Flow. Research Report, K-Water, Korea.

Kang, 2012. Comparison of physical habitat suitability index for fishes in the rivers of Han and Geum River Watersheds. *Korean Soc. Civil Eng.* 32, 71–78. <https://doi.org/10.12652/Ksce.2012.32.1B.071>.

Kellerhals, R., Miles, M., 1996. Fluvial geomorphology and fish habitat: implications for river restoration. In: *Ecohydraulics 2000: Proceedings 2nd International Symposium on Habitat Hydraulics*, Quebec, 1996.

Khosronejad, A., Kang, S., Borazjani, I., Sotiroopoulos, F., 2011. Curvilinear immersed boundary method for simulating coupled flow and bed morphodynamics interactions due to sediment transport phenomena. *Adv. Water Resour.* 34, 829–843. <https://doi.org/10.1016/j.advwatres.2011.02.017>.

Kim, S.K., Choi, S.-U., 2021. Assessment of the impact of selective withdrawal on downstream fish habitats using a coupled hydrodynamic and habitat modeling. *J. Hydrol.* 593, 125665. <https://doi.org/10.1016/j.jhydrol.2020.125665>.

K-water, 2023. Hydrologic Data. My Water: Water Information Portal. Available from: https://www.water.or.kr/kor/realtime/sumun/index.do?mode=sumun&menuId=_13_91_93_94 (accessed 24 October 2024).

Lai, Yong G., 2020. A two-dimensional depth-averaged sediment transport mobile-bed model with polygonal meshes. *Water* 12, 1032. <https://doi.org/10.3390/w12041032>.

Lai, Y.G., Liu, X., Bombardelli, F.A., Song, Y., 2022. Three-dimensional numerical modeling of local scour: a state-of-the-art review and perspective. *J. Hydraul. Eng. ASCE* 148, 03122002. [https://doi.org/10.1061/\(ASCE\)HY.1943-7900.0002019](https://doi.org/10.1061/(ASCE)HY.1943-7900.0002019).

Ministry of Environment, 2022. Report for the Basic River Plan in Upper Geum-Gang River System [In Korean], Republic of Korea.

Ministry of Land, Infrastructure, and Transport, 2011. Report for the Basic River Plan in Geum-Gang River System [In Korean], Republic of Korea.

Parker, G., 2004. *1D Sediment Transport Morphodynamics with Applications to Rivers and Turbidity Currents*, e-Book.

Parra, T.S., Politti, E., Zolezzi, G., 2024. Morphological and fish mesohabitat dynamics following an experimental flood under different sediment availability. *Earth Surf. Process. Landf.* 49 (15), 5167–5185. <https://doi.org/10.1002/esp.6025>.

Parsapour-Moghaddam, P., Brennan, C.P., Rennie, C.D., Elvidge, C.K., Cooke, S.J., 2019. Impacts of channel morphodynamics on fish habitat utilization. *Environ. Manag.* 64, 272–286. <https://doi.org/10.1007/s00267-019-01197-0>.

Servanzi, L., Quadroni, S., Espa, P., 2024. Hydro-morphological alteration and related effects on fish habitat induced by sediment management in a regulated Alpine river. *Int. J. Sediment Research* 39 (4), 514–530. <https://doi.org/10.1016/j.ijsrc.2023.10.001>.

Simon, A., Thomas, R.E., Curini, A., Shields Jr., F.D., 2002. Case study: channel stability of the Missouri River, Eastern Montana. *J. Hydraul. Eng. ASCE* 128, 880–890. [https://doi.org/10.1061/\(ASCE\)0733-9429\(2002\)128:10\(880\)](https://doi.org/10.1061/(ASCE)0733-9429(2002)128:10(880).

USACE, 2024. HEC-RAS Documentation, Hydrologic Engineering Center. <https://www.hec.usace.army.mil/software/hec-ras/documentation.aspx>.

White, J.S., Bartelt, K., Overstreet, B.T., Kelley, J.R., 2025. High resolution mapping of submerged sediment size and suitable salmon spawning habitat using topographic Lidar in the Santiam River basin, Oregon. *Water Resour. Res.* 61 (8), e2024WR039219. <https://doi.org/10.1029/2024WR039219>.

Woo, H., 2001. *River Hydraulics*. Cheongmoongak Press, Seoul, Korea (in Korean).

Woo, H., 2010. Trends in ecological river engineering in Korea. *J. Hydro Environ. Res.* 4 (4), 269–278. <https://doi.org/10.1016/j.jher.2010.06.003>.

Yang, G., Bao, M., Cong, N., Kattel, G., Li, Y., Xi, Y., Wang, Y., Wang, Q., Yao, W., 2023. Application of a fish habitat model to assess habitat fragmentation using high flow and sediment transport in the Rumei Dam in Lancang River (China). *Ecohydrology* 17 (4), e2583. <https://doi.org/10.1002/eco.2583>.